BIOCHEMISTRY
including biophysical chemistry & molecular biology

Article

pubs.acs.org/biochemistry

Modification of Interdomain Interfaces within the A3C1C2 Subunit of Factor VIII Affects Its Stability and Activity

Hironao Wakabayashi and Philip J. Fay*

Department of Biochemistry and Biophysics, University of Rochester School of Medicine, 601 Elmwood Avenue, Rochester, New York 14642, United States

ABSTRACT: Factor (F)VIII consists of a heavy chain [A1(a1)A2(a2)B domains] and a light chain [(a3)A3C1C2 domains]. Several reports have shown significant changes in FVIII stability and/or activity following selected mutations at the A1−A2, A1−A3, A2−A3, and A1−C2 domain interfaces. In this study, the remaining inter-FVIII subunit interfaces (A3−C1 and C1−C2) were examined for their contributions to the stability and activity of FVIII and FVIIIa. We prepared FVIII mutants with nascent disulfide bridges between A3 and C1 domains (Gly1750Cys/Arg2116Cys and Ala1866Cys/Ser2119Cys) or C1 and C2 domains (Ser2029Cys/Pro2292Cys). We also prepared mutants via replacement of Arg2116 with hydrophobic residues (Ala and Val) because this C1 domain residue appears to face a pocket of positive electrostatic potential in the A3 domain. Stability was assessed following the rates of loss of FVIII activity at 55 °C and the spontaneous loss of FVIIIa activity from A2 subunit dissociation. FVIII Gly1750Cys/Arg2116Cys showed a marked increase in thermal stability (~3.7-fold) compared with that of wild-type (WT) FVIII, while the stability of FVIII Ala1866Cys/Ser2119Cys was reduced (~4.7-fold). Although the Ser2029Cys/Pro2292Cys variant showed a modest loss of FVIII stability, the specific activity and thrombin generation potential of this variant were increased (up to 1.2-fold) compared with those of WT. Furthermore, this variant demonstrated an ~2-fold reduced K_m for FX. Mutation of Arg2116 to hydrophobic residues resulted in variable decreases in stability and thrombin generation parameters, suggesting a role of this Arg residue contributing to FVIII structure. Taken together, selective modification of the contiguous domain interfaces in the FVIII light chain may improve FVIII stability and/or cofactor function.

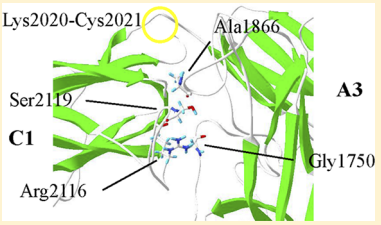

Factor VIII (FVIII), a plasma protein that is present at a decreased level or is defective in individuals with hemophilia A, is expressed as both single-chain and heterodimer forms. The latter consists of a heavy chain (HC) comprised of A1(a1)A2(a2)B domains and a light chain (LC) comprised of (a3)A3C1C2 domains, with the lower case a representing short (~30−40 residue) segments rich in acidic residues (see ref 1 for a review). FVIII is activated by proteolytic cleavages at the a1A2, a2B, and a3A3 junctions catalyzed by thrombin or factor Xa. The resulting product, FVIIIa, is a heterotrimer comprised of subunits designated A1, A2, and A3C1C2 that functions as a cofactor for the serine protease FIXa in the membrane-dependent conversion of zymogen FX to the serine protease, FXa (see ref 1 for a review).

Reconstitution studies have shown that the FVIII heterodimeric structure is supported by both electrostatic and hydrophobic interactions.[2] Metal ions also contribute to the interchain affinity and activity parameters.[3] Occupancy of a calcium site in the A1 domain (110−126) is required to yield the active FVIII conformation.[4] Copper ions facilitate the association of HC and LC to form the heterodimer, increasing the interchain affinity by severalfold at physiologic pH.[5,6] Intermediate-resolution X-ray structures of FVIII[7,8] showed occupancy of a calcium site in the A1 domain and the two type 1 copper ion sites within the A1 and A3 domains.

The instability of FVIIIa results from weak electrostatic interactions between the A2 subunit and the A1/A3C1C2 dimer,[9,10] and its dissociation leads to a decrease in FXase activity.[11,12]

Examination of hydrogen bonding interactions at the A1−A2 and A2−A3 interfaces following mutation of selected charged or polar residues spatially separated by <2.8 Å showed loss of function, as judged by increased rates of FVIII decay at 55 °C and/or rates for FVIIIa decay relative to that of the wild type (WT), in approximately half of the 30 residues tested,[13] suggesting that multiple residues at the A1−A2 and A2−A3 domain interfaces contribute to the stabilization of FVIII.

Mutations to increase the buried hydrophobic area and/or decrease the buried hydrophilic area often result in enhanced protein stability.[14] Earlier studies showed that acidic residues localized to hydrophobic pockets at the A1−A2 interface (Asp519) and A2−A3 interface (Glu665 and Glu1984) upon mutation to hydrophobic residues (Ala or Val), had favorable effects on FVIII/FVIIIa stability and/or activity.[15,16] In addition, replacing Ala108 that localized to a hydrophobic pocket at the A1−C2 domain interface with the more bulky Ile also caused a marked increase in FVIII stability.[17] Furthermore, introducing nascent disulfide bridges between FVIII subunits by double Cys mutation at A2−A3 or A1−C2 interfaces yielded FVIII variants with enhanced FVIII/FVIIIa stability.[17−19]

Received: March 7, 2013
Revised: May 8, 2013
Published: May 9, 2013

   dx.doi.org/10.1021/bi400295x | *Biochemistry* 2013, 52, 3921−3929

Although the A3C1C2 domains are covalently linked in the FVIII light chain, the FVIII X-ray crystal structure suggests the A3−C1 and C1−C2 domain interfaces are maintained by noncovalent interactions.[7,8] In this study, we examined the effect of generating additional covalent and noncovalent interactions at the A3−C1 and C1−C2 interfaces. Results show that a selected A3−C1 interface modification is favorable for FVIII stability and a C1−C2 interface modification enhanced cofactor function likely by reducing the K_m of FXase for substrate factor X. In addition, these results reveal a role for C1 residue Arg2116 in maintaining FVIII stability.

MATERIALS AND METHODS

Reagents. Recombinant FVIII (Kogenate) and monoclonal anti-A3 antibody 2D2 were generous gifts from L. Regan of Bayer Corp. (Berkeley, CA). Phospholipid vesicles containing 20% phosphatidylcholine (PC), 40% phosphatidylethanolamine (PE), and 40% phosphatidylserine (PS) were prepared using octyl glucoside as described previously.[20] The reagents α-thrombin, FVIIa, FIXaβ, FX, and FXa (Enzyme Research Laboratories, South Bend, IN), hirudin and phospholipids (DiaPharma, West Chester, OH), the chromogenic FXa substrate, Pefachrome Xa (Pefa-5523, CH_3OCO-D-CHA-Gly-Arg-pNA·AcOH; Centerchem Inc., Norwalk CT), recombinant human tissue factor (rTF), Innovin (Dade Behring, Deerfield, IL), fluorogenic substrate, Z-Gly-Gly-Arg-AMC (Calbiochem, San Diego, CA), thrombin calibrator (Diagnostica Stago, Parsippany, NJ), and Enhanced Chemifluorescence reagent (GE Healthcare Bioscience, Piscataway, NJ) were purchased from the indicated vendors.

Construction, Expression, and Purification of WT and Variant FVIII. WT FVIII and variants with double mutations (Gly1750Cys/Arg2116Cys, Ala1866Cys/Ser2119Cys, and Ser2029Cys/Pro2292Cys) and single mutations (Arg2116Ala and Arg2116Val) were individually constructed as B-domainless FVIII, lacking residues Gln744−Ser1637 in the B-domain.[21] Recombinant WT and variant FVIII forms were stably expressed in BHK cells and purified as described previously.[4] Protein yields for the variants ranged from >10 to ∼100 μg from two 750 cm^2 culture flasks, with purities from ∼85 to >95% as judged by SDS−PAGE. The primary contaminant in the FVIII preparations was albumin. The FVIII concentration was measured using an enzyme-linked immunoadsorbant assay (ELISA), and FVIII activity was determined by one-stage clotting and two-stage chromogenic FXa generation assays described below.

ELISA. A sandwich ELISA was performed as previously described[22] using purified commercial recombinant FVIII (Kogenate, Bayer Corp.) as a standard. FVIII capture used the anti-C2 antibody (GMA8003, Green Mountain Antibody, Burlington, VT), and the R8B12 antibody (Green Mountain Antibody) was employed for FVIII detection following its biotinylation.

FVIII Activity and Stability Measurements. One-stage clotting assays were performed using substrate plasma chemically depleted of FVIII as previously described.[15] The rate of conversion of FX to FXa was monitored in a purified system according to a two-stage FXa generation assay previously described.[15] FVIII activity decay at elevated temperatures (55 °C) was measured by incubating WT or variant FVIII (4 nM) in 20 mM *N*-(2-hydroxyethyl)piperazine-*N*′-2-ethanesulfonic acid (HEPES) (pH 7.2), 0.1 M NaCl, 0.01% bovine serum albumin, and 0.01% Tween 20 (buffer A) and monitoring residual FVIII activity using an FXa generation assay. The spontaneous decay of FVIIIa activity was measured following activation of WT or mutant FVIII (1.5 nM) by thrombin (20 nM) for 1 min in the absence or presence of FIXa (10 nM), followed by addition of hirudin (10 units/mL) to inactivate thrombin. Residual activity was determined using the FXa generation assay. Data were fit to the single-exponential decay equation by nonlinear least-squares regression, and parameter values were obtained.

Michaelis−Menten Kinetics and FIXa Binding Affinity. FVIII (1 nM) in buffer A containing 10 μM PSPCPE vesicles was activated by 20 nM thrombin for 1 min and immediately reacted with hirudin (10 units/mL) and 40 nM FIXa, and FXa generation was initiated by adding the indicated concentrations of FX. Measurement of the binding affinity of FVIIIa for FIXa was performed as follows. FVIII (1 nM) in buffer A containing 10 μM PSPCPE vesicles was activated by 20 nM thrombin for 1 min and immediately reacted with hirudin (10 units/mL) and the indicated concentrations of FIXa, and FXa generation was initiated by adding 300 nM FX as described above. Data were fit to the Michaelis−Menten equation or the steady state binding equation by nonlinear least-squares regression, and parameter values were obtained.

Western Blotting. FVIIIa proteins prepared following activation of FVIII (0.34 μg) by thrombin (20 nM) for 30 min at 23 °C were subjected to electrophoresis under reducing (0.1 M dithiothreitol) and nonreducing conditions using 6% polyacrylamide gels at a constant voltage (150 V). Proteins were transferred to a polyvinylidene fluoride membrane and probed with an anti-A3 domain monoclonal antibody (2D2), and protein bands were visualized by chemifluorescence using a Gel Doc XR+ System (Bio-Rad, Hercules, CA).

Thrombin Generation Assay. The amount of thrombin generated in plasma was measured by Calibrated Automated Thrombography[23] using methods previously described.[15] Briefly, FVIII deficient plasma (<1% residual activity, platelet-poor) from a severe hemophilia A patient lacking FVIII inhibitor (George King Bio-Medical, Overland Park, KS) was mixed at 37 °C with final concentrations of 0.25 nM FVIII, 0.5 pM rTF, 4 μM PSPCPE vesicles, 433 μM fluorogenic substrate, 13.3 mM $CaCl_2$, and 105 nM thrombin calibrator. The development of a fluorescence signal was monitored at 8 s intervals using a microplate spectrofluorometer (Spectramax Gemini, Molecular Devices, Sunnyvale, CA) with a 355 nm (excitation)/460 nm (emission) filter set. Fluorescence signals were corrected by the reference signal from the thrombin calibrator samples,[23] and actual thrombin generation in nanomolar was calculated as previously described.[15]

Data Analysis. FVIII/VIIIa activity values as a function of time were fit to a single-exponential decay curve by nonlinear least-squares regression using the equation

$$A = A_0 e^{-kt}$$

where A is the residual FVIIIa activity (nanomolar per minute per nanomolar FVIII), A_0 is the initial activity, k is the apparent rate constant, and t is the time (minutes) of reaction of either FVIII at 55 °C (for FVIII decay experiments) or after thrombin activation had been quenched (for FVIIIa decay measurements).

For Michaelis−Menten kinetics or FIXa binding affinity measurements, we used the following equation

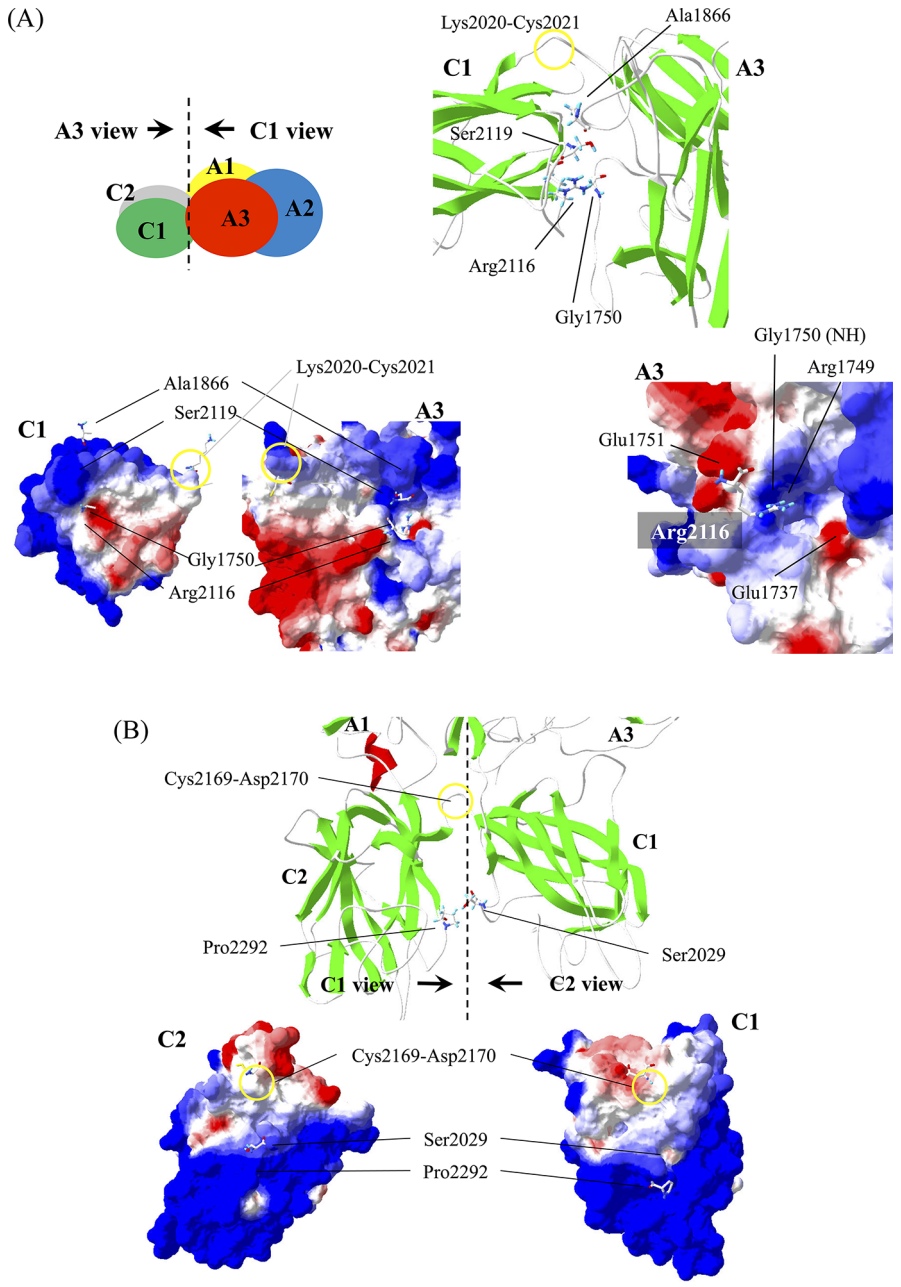

Figure 1. (A) Interface structure with selected residues at the A3−C1 domain interface. In the top left panel, a cartoon of FVIII was drawn based on the crystal structure[8] with the A1 domain (residues 1−336) colored yellow, the A2 domain (residues 373−711) blue, the A3 domain (residues 1690−2020) red, the C1 domain (residues 2021−2169) green, and the C2 domain (residues 2170−2332) gray. Each molecular surface of the interface is viewed in the direction of the arrow and is shown in the bottom left panel. In the bottom left panel, electrostatic potential was calculated with Swiss PDB viewer with a simple coulomb interaction mode using a uniform dielectric constant (80) and is colored red (negative) or blue (positive). Residues facing A3 and C1 surfaces are drawn as sticks. The top right panel shows a higher-magnification image of the A3−C1 contact region drawn as ribbons. The Lys2020−Cys2021 covalent bond is indicated by a yellow circle. Several indicated key residues are drawn as sticks. The bottom right panel shows a higher-magnification image of the A3 surface with electrostatic potential. Arg2116 from C1 is drawn as sticks. (B) Interface structure with selected residues at the C1−C2 domain interface. The top panel shows a higher-magnification image of the C1−C2 contact region as ribbons. The Cys2169−Asp2170 covalent bond is indicated by a yellow circle. Ser2029 and Pro2292 are drawn as sticks. Each molecular surface of the interface is viewed in the direction of the arrow and is shown in the bottom panel. The bottom panel shows the molecular surface with electrostatic interaction of C1 (right) and C2 (left). Residues facing C1 and C2 surfaces are drawn as sticks. In the stick models, hydrogen, carbon, oxygen, nitrogen, and sulfur are colored cyan, white, red, blue, and yellow, respectively. Ribbon structures represent α-helix (red) and β-strand (green).

$$A = \frac{V_{max}X}{K + X}$$

where A is the initial velocity of FXa generation (nanomolar per minute per nanomolar FVIII), X is the FX or FIXa concentration, K is the Michaelis constant (K_m) or dissociation constant (K_d), and V_{max} is the maximal activity at a saturating substrate concentration.

Nonlinear least-squares regression analysis was performed using a standard curve-fitting algorithm (the Gauss−Newton

dx.doi.org/10.1021/bi400295x | *Biochemistry* 2013, 52, 3921−3929

Table 1. Factor VIII Activity and Stability Data[a]

	clotting (units/μg)	FXa generation assay [nM FXa min^{-1} (nM FVIII)$^{-1}$]	FVIII decay rate constant (min^{-1})	FVIIIa decay rate constant (min^{-1})	
				without FIXa	with FIXa
WT	4.61 ± 0.30 (1.00)	44.8 ± 0.8 (1.00)	0.0423 ± 0.0013 (1.00)	0.121 ± 0.012 (1.00)	0.018 ± 0.001 (1.00)
G1750C/R2116C	3.03 ± 0.11 (0.66)	26.1 ± 1.5 (0.58)	0.0118 ± 0.0014 (0.28)	0.089 ± 0.003 (0.74)	0.018 ± 0.001 (1.00)
A1866C/S2119C	1.37 ± 0.17 (0.30)	13.3 ± 0.8 (0.30)	0.1995 ± 0.0089 (4.71)	0.132 ± 0.004 (1.09)	0.019 ± 0.002 (1.06)
R2116A	4.81 ± 0.06 (1.04)	47.0 ± 1.3 (1.05)	0.2144 ± 0.0093 (5.07)	0.151 ± 0.008 (1.25)	0.017 ± 0.001 (0.94)
R2116V	4.04 ± 0.05 (0.88)	28.3 ± 0.5 (0.63)	0.0760 ± 0.0044 (1.80)	0.156 ± 0.009 (1.29)	0.018 ± 0.002 (1.00)
S2029C/P2292C	5.39 ± 0.10 (1.17)	37.8 ± 1.5 (0.85)	0.1572 ± 0.0118 (3.71)	0.140 ± 0.012 (1.16)	0.015 ± 0.001 (0.83)

[a]FVIII activity determined by one-stage clotting and two-stage FXa generation assays and FVIII/FVIIIa stability determined by FVIII thermal activity decay at 55 °C and FVIIIa spontaneous activity decay at 23 °C (in the presence or absence of FIXa) were measured as described in Methods. Activity and decay parameter values ± the standard deviation were calculated as described in Methods. Data represent the average values of triplicate samples. Values in parentheses are relative to the WT value. The single-letter code is used to designate amino acid residues: G, Gly; R, Arg; A, Ala; S, Ser; C, Cys; V, Val; P, Pro.

algorithm with the Levenberg–Marquardt method). Comparison of average values was performed by the Student's t test.

RESULTS

Generation of FVIII Variants with Nascent Disulfide Bridging at the A3–C1 and C1–C2 Domain Interfaces and Arg2116 Point Mutants. The A3C1C2 subunit of FVIIIa is a single-chain protein with domains delineated by residues Lys2020 and Cys2021 (A3–C1) and Cys2169 and Asp2170 (C1–C2) (see Figure 1). In addition to covalent attachment, the interdomain interfaces show potential for significant noncovalent interactions. Figure 1A illustrates the A3–C1 interface and identifies two residues, Ala1866 and Gly1750, in the A3 domain that are in the proximity of C1 domain residues Ser2119 and Arg2116, respectively (Cα distances of 6.5 and 5.4 Å, respectively[8]). In an attempt to increase the stability of this region, these paired residues (Ala1866/Ser2119 and Gly1750/Arg2116) were mutated to Cys to form additional covalent linkages through nascent disulfide bonding. In addition, we noted that C1 residue Arg2116 resides at the interdomain interface in the proximity of an area of basic electrostatic potential in the A3 domain. Because this interaction could be destabilizing to A3–C1 domain interactions, we mutated this residue to either Ala or Val. Finally, examination of the C1–C2 domain interface (Figure 1B) indicated the proximity of C1 domain residue Ser2029 to C2 domain residue Pro2292 (Cα distance of 7.3 Å[8]), and these residues were mutated to Cys in an effort to disulfide bridge the two C domains. While the FVIII variants described above could be expressed in BHK cells, we noted that other pairings used in attempts to produce disulfide bridges linking A3 and C1 domains (Glu1751Cys/Pro2142Cys, Leu1752Cys/Asn2118Cys, Leu1752Cys/Pro2142Cys, His1867Cys/Ser2119Cys, and Val1933Cys/Pro2143Cys) or C1 and C2 domains (Ser2029Cys/Val2293Cys and Ser2029Cys/Val2294Cys) were not expressed in cell culture.

Specific activity values of purified FVIII proteins were measured by both one-stage and two-stage assays, and data are listed in Table 1. FVIII Gly1750Cys/Arg2116Cys retained ~60% of the specific activity of FVIII WT, whereas that of Ala1866Cys/Ser2119Cys was reduced to ~30% of the WT value. The C1–C2 interface mutant (Ser2029Cys/Pro2292Cys) and point mutants Arg2116Ala and Arg2116Val possessed specific activity values near the WT value.

The formation of disulfide bonds was assessed by comparison of the electrophoretic mobility of the variants with that of WT A3C1C2. Figure 2 shows SDS–PAGE of the A3C1C2 subunits of WT FVIII and variants as detected by an anti-A3 domain monoclonal antibody (2D2). Under reducing conditions (0.1 M dithiothreitol), WT and variant A3C1C2 subunits showed equivalent mobility migrating to the same position (~70 kDa, lanes 1–4) on the gel. However, under nonreducing conditions, the A3C1C2 subunits from disulfide-bridged variants Gly1750Cys/Arg2116Cys (lane 6), Ala1866-Cys/Ser2119Cys (lane 7), and Ser2029Cys/Pro2292Cys (lane 8) migrated faster than WT A3C1C2 (lane 5). These results are consistent with the presence of an additional covalent bridge in the subunit yielding a tighter intersubunit conformation.

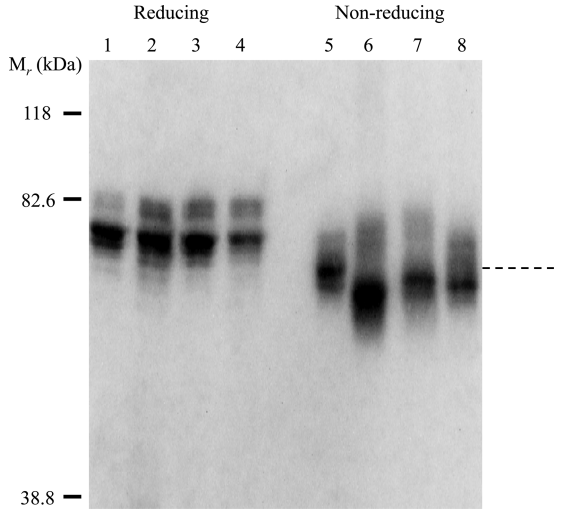

Figure 2. Western blot analysis of WT FVIII and variants. Thrombin-activated WT and mutant FVIIIa proteins were electrophoresed under reducing (lanes 1–4) or nonreducing (lanes 5–8) conditions, transferred, and probed with 2D2 (anti-A3 domain monoclonal antibody). Protein bands were visualized by chemifluorescence as described in Methods. Shown are WT (lanes 1 and 5), Gly1750Cys/Arg2116Cys (lanes 2 and 6), Ala1866Cys/Ser2119Cys (lanes 3 and 7), and Ser2029Cys/Pro2292Cys (lanes 4 and 8) FVIII proteins.

Stability of FVIII Variants. The FVIII thermal decay assay at 55 °C as measured by the FXa generation assay represents the stability of intersubunit interaction.[6] Figure 3 shows the results of thermal decay at 55 °C for WT FVIII and its variants. Among the mutants tested, only Gly1750Cys/Arg2116Cys showed an increased thermal stability, retaining ~70% activity at ~35 min after heat challenge as compared with WT, which

dx.doi.org/10.1021/bi400295x | Biochemistry 2013, 52, 3921–3929

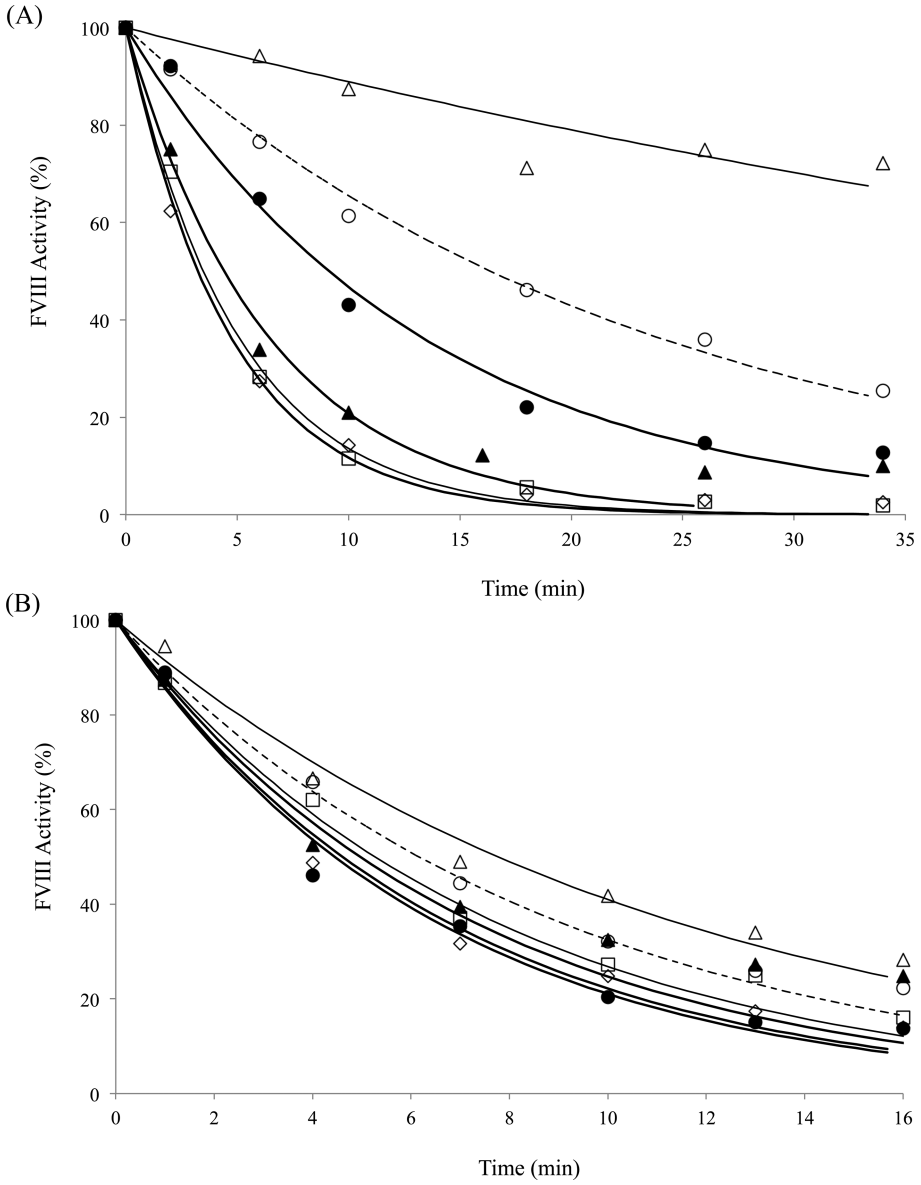

Figure 3. (A) FVIII activity decay at elevated temperatures. FVIII (4 nM) was incubated at 55 °C, and at the indicated times, aliquots were removed and activity was measured by FXa generation assays as described in Methods. Data were fit to a single-exponential decay curve by nonlinear least-squares regression, and lines were drawn. (B) FVIIIa decay. Thrombin-activated FVIIIa (1.5 nM) was incubated at 23 °C; aliquots were taken at the indicated time points, and activity was measured by the FXa generation assay as described in Methods. Data were fit to a single-exponential decay curve by nonlinear least-squares regression, and lines were drawn. Symbols denote WT (−−○−−), Gly1750Cys/Arg2116Cys (△), Ala1866Cys/Ser2119Cys (□), Arg2116Ala (◇), Arg2116Val (●), and Ser2029Cys/Pro2292Cys (▲). Each point represents the value averaged from three separate determinations.

was reduced to <70% activity in 10 min (Figure 3A). The calculated decay rate for this variant was reduced by ∼3.6-fold compared with the WT FVIII value (Table 1), and this result is consistent with the additional disulfide bridge at the A3−C1 interface stabilizing the FVIII structure. Alternatively, the Ala1866Cys/Ser2119Cys variant, which also possesses an added disulfide bridge at this interface, yielded a faster decay than WT with <20% activity remaining in 10 min (Figure 3A). The calculated decay rate for this variant was ∼4.7-fold greater than the WT value (Table 1). These results indicate markedly different effects on FVIII stability depending on the location of the added linkage within the A3−C1 interface. FVIII variants with point mutations at Arg2116 showed thermal decay rates faster than that of WT, with the Arg2116Ala mutation yielding an ∼5-fold increase in rate and the Arg2116Val mutation yielding a nearly 2-fold increase in rate (Figure 3A and Table 1). These results indicate that the Arg residue at this site in native FVIII likely contributes favorable interaction(s) to FVIII structure in stabilizing the domain interface, whereas the hydrophobic Ala or Val at this position is destabilizing. The decay rate of the C1−C2 interface mutant (Ser2029Cys/Pro2292Cys) was also faster than that of WT, showing ∼20% activity remaining after 10 min at the elevated temperature (Figure 3A), which was estimated to be an ∼3.7-fold increase compared with that of WT FVIII (Table 1).

FVIIIa activity decay is governed by the dissociation of the A2 subunit, which interacts with the A1 subunit and A3 domain of the A3C1C2 subunit. Because these interactive sites are far

dx.doi.org/10.1021/bi400295x | *Biochemistry* 2013, 52, 3921−3929

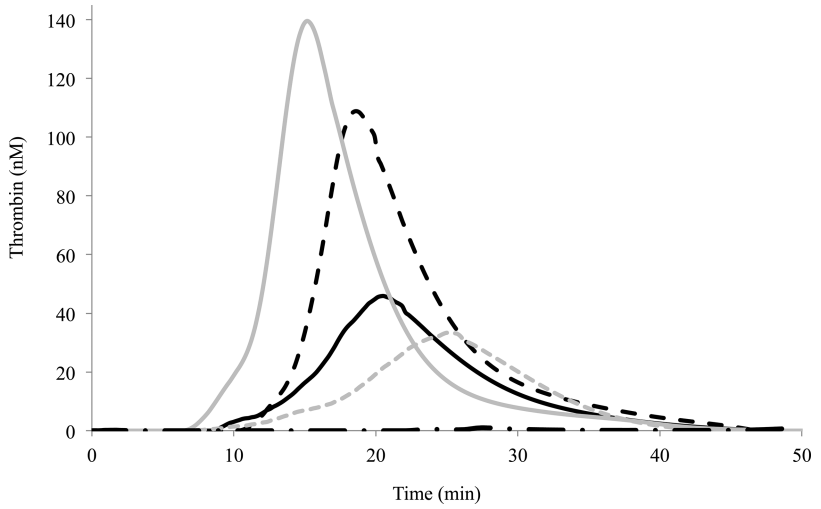

Figure 4. Thrombin generation assay. Thrombin generation assays were performed in the presence of 0.25 nM WT FVIII or variant, 0.5 pM rTF, and 4 μM PSPCPE vesicles. Data represent the average values of triplicate samples. Representative thrombograms of WT (black dotted line), Gly1750Cys/Arg2116Cys (black solid line), Ala1866Cys/Ser2119Cys (gray dotted line), Ser2029Cys/Pro2292Cys (gray solid line), and a negative control (0 nM FVIII, black alternate dashed−dotted line) are shown.

Table 2. Thrombin Generation Assay Parameter Values[a]

	latent time (min)	peak time (min)	peak value (nM)	ETP (nM/min)
WT	11.9 ± 0.2 (1.00)	18.6 ± 0.1 (1.00)	108.9 ± 9.1 (1.00)	957.9 ± 41.1 (1.00)
G1750C/R2116C	11.5 ± 1.2 (0.97)	20.6 ± 1.0 (1.11)	45.9 ± 4.5 (0.42)	514.2 ± 19.7 (0.54)
A1866C/S2119C	13.2 ± 3.5 (1.11)	25.1 ± 2.7 (1.35)	33.4 ± 1.5 (0.31)	408.8 ± 36.5 (0.43)
R2116A	10.4 ± 0.2 (0.87)	18.2 ± 0.1 (0.98)	76.5 ± 8.6 (0.70)	744.1 ± 91.3 (0.78)
R2116V	12.6 ± 0.2 (1.06)	18.6 ± 0.1 (1.00)	69.4 ± 3.5 (0.64)	595.4 ± 4.4 (0.62)
S2029C/P2292C	7.8 ± 0.7 (0.66)	15.1 ± 0.3 (0.81)	139.6 ± 12.8 (1.28)	1076.0 ± 24.0 (1.12)

[a]Thrombin generation assays in the presence of 0.25 nM FVIII proteins, 0.5 pM rTF, and 4 μM PSPCPE vesicles were performed, and parameter values were calculated as described in Methods. Data represent the average values ± the standard deviation of triplicate samples. Values in parentheses are relative to the WT value. The single-letter code is used to designate amino acid residues: G, Gly; R, Arg; A, Ala; S, Ser; C, Cys; V, Val; P, Pro.

removed from the A3−C1 and C1−C2 domain interfaces, we did not expect to observe large changes in FVIIIa stability with the variants. Although its stability was modest, the Gly1750Cys/Arg2116Cys variant possessed an improved FVIIIa stability showing an activity value retaining 5−10% more than the WT after a 10 min incubation (Figure 3B). The estimated FVIIIa decay rate for this variant was ∼30% slower than that of WT FVIII (Table 1; $p < 0.05$). Interestingly, in the presence of FIXa (10 nM), the FVIIIa decay rate was slower but similar to that of WT FVIII (Table 1), suggesting that the effect of this mutation on FVIIIa stability can be substituted by FIXa. FVIIIa decay profiles for the Ala1866Cys/Ser2119Cys variant and the two Arg2116 mutants were similar to that of the WT in the absence of FIXa, and the value was lower and approached the WT value in the presence of FIXa (Table 1). Thrombin-activated Ser2029Cys/Pro2292Cys FVIIIa decayed slightly faster than WT FVIIIa, showing an ∼1.2-fold increase in the decay rate compared with that of the WT; however, in the presence of FIXa, the decay rate was ∼1.2-fold lower than the WT value (Table 1). The data described above suggest that modifications at the A3−C1 and C1−C2 domain interfaces result in generally minimal effects relative to A2 subunit retention.

Thrombin Generation. FVIII variant activity was assessed by thrombin generation assays performed at a low rTF concentration (0.5 pM) using FVIII deficient plasma. Figure 4 shows a representative thrombogram of WT FVIII and selected variants with parameter values listed in Table 2. Thrombin generation with WT FVIII was initiated at ∼12 min, and peak thrombin generation (∼110 nM) was reached at ∼19 min. The FVIII Gly1750Cys/Arg2116Cys and Ala1866Cys/Ser2119Cys variants showed reductions in the extent of thrombin generation with ETP values that were 54 and 43% of the WT value, respectively. These values were compatible with the observed specific activity values (∼60 and 30%, respectively) for the two variants. Furthermore, we observed a significant delay for thrombin generation parameters (∼10% in latent time and ∼30% in peak time relative to WT) for the Ala1866Cys/Ser2119Cys variant. On the other hand, the Ser2029Cys/Pro2292Cys variant linking C1 and C2 domains showed somewhat improved thrombin generation (112% ETP value as compared with the WT FVIII value; $p < 0.05$), which again corresponded to the increased specific activity (117% by a one-stage assay) of this variant. Furthermore, latent and peak times were significantly shortened (∼20 and 35%, respectively) relative to that of the WT. Thrombin generation using the Arg2116Ala and -Val mutants showed ∼30% reductions in peak and ETP values compared with WT values. In addition, we performed experiments to measure thrombin activation of FVIII under conditions where excess FVIII (20 nM) was activated by 0.5 nM thrombin, and the rate of FVIIIa generation was measured as an initial velocity during a 1 min reaction in 10 s intervals. All of the mutants showed efficiencies similar to those of WT FVIII (within a 20% difference). The

dx.doi.org/10.1021/bi400295x | *Biochemistry* 2013, 52, 3921−3929

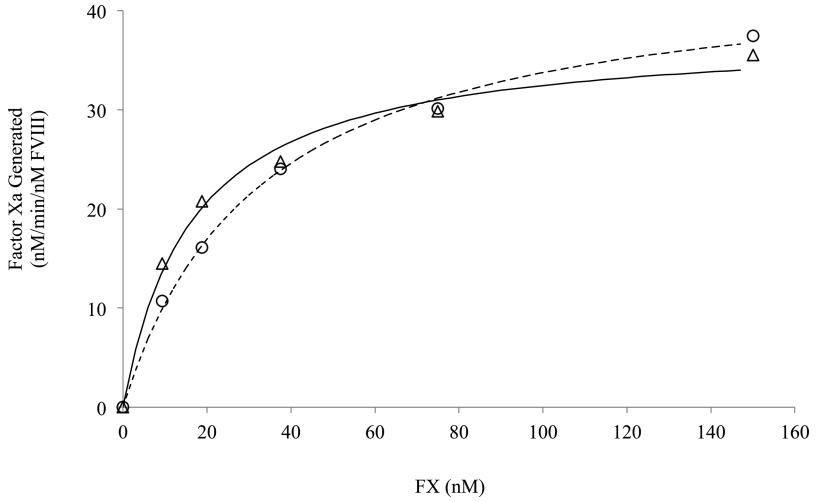

Figure 5. Michaelis–Menten analysis of the FXase complex. FVIII (1 nM) was activated by 20 nM thrombin for 1 min and immediately reacted with hirudin (10 units/mL) and 40 nM FIXa, and FXa generation was initiated by adding the indicated concentrations of FX. The rate of generated FXa was measured as described in Methods. Data were fit to the Michaelis–Menten equation by nonlinear least-squares regression, and fitted lines were drawn. Each point represents the value averaged from three separate determinations: WT (○) and Ser2029Cys/Pro2292Cys (△).

rate values were 34.7 ± 0.69, 36.1 ± 1.21, 33.6 ± 1.16, 41.3 ± 2.70, and 33.6 ± 1.89 nM FVIIIa generated per minute per nanomolar thrombin for WT FVIII, Gly1750Cys/Arg2116Cys, Ala1866Cys/Ser2119Cys, Arg2116Ala, and Arg2116Val, respectively. Furthermore, WT FVIII and its variants show similar affinities for FIXa (within a 10% difference). K_d values were 0.43 ± 0.02, 0.44 ± 0.05, 0.40 ± 0.04, 0.45 ± 0.05, and 0.40 ± 0.06 nM for WT FVIII, Gly1750Cys/Arg2116Cys, Ala1866Cys/Ser2119Cys, Arg2116Ala, and Arg2116Val, respectively. Overall, the reason for the modestly reduced thrombin generation profile of the Arg2116 mutants is not clear but may reflect the slightly increased FVIIIa decay rate observed in the absence of FIXa.

FVIII Function Analyses of the WT and Ser2029Cys/Pro2292Cys Variant. To gain insights into the increased specific activity (by a one-stage assay) and thrombin generation potential of the Ser2029Cys/Pro2292Cys variant relative to that of the WT, we examined functional interactions of the cofactor with FIXa and FX. For interactions with FIXa, WT FVIII (1 nM) or a variant was activated by thrombin and titrated with various concentrations of FIXa, and rates of FXa generation were measured as described in Methods. FXa generation curves for WT and the Ser2029Cys/Pro2292Cys variant were hyperbolic and could be saturated with FIXa (data not shown). From the fitted curves, K_d values of 0.43 ± 0.02 and 0.33 ± 0.04 nM were determined for WT and the Ser2029Cys/Pro2292Cys variant, respectively. These results suggest the WT and variant show similar affinities for FIXa. Thrombin (0.5 nM) activation measurements of FVIII (20 nM) also showed similar values for the WT and the Ser2029Cys/Pro2292Cys variant (34.7 ± 0.69 and 38.5 ± 1.11 nM FVIIIa generated per minute per nanomolar thrombin, respectively).

Michaelis–Menten kinetics were used to assess the FVIIIa-dependent interaction of FX with the FXase complex. The rate of generation of FXa with 1 nM FXase (1 nM FVIII activated by thrombin and reacted with 40 nM FIXa) was performed at various concentrations of FX as described in Methods. Results are shown in Figure 5. Both WT and Ser2029Cys/Pro2292Cys FVIII generated FXa at rates that were saturable, showing hyperbolic titration curves with an increasing FX concentration. The estimated V_{max} values were 44.8 ± 1.3 and 37.8 ± 1.5 nM/min for the WT and Ser2029Cys/Pro2292Cys, respectively. Interestingly, the K_m value for the mutant was approximately one-half of the WT value (32.8 ± 2.6 and 16.5 ± 2.4 nM for WT and Ser2029Cys/Pro2292Cys FVIII, respectively; $p < 0.005$). The reduced K_m for FX observed for the disulfide-bridged variant likely contributes in part to the modest increase in activity observed in the one-stage and thrombin generation assays where plasma concentrations of FX are present.

■ DISCUSSION

Previously, we reported that mutagenesis of selected residues at the A1–A2, A2–A3, A1–A3, and A1–C2 domain interfaces variably affected, both positively and negatively, FVIII and/or FVIIIa stability.[6,13,16,17,24] In the study presented here, we extend this line of investigation to the remaining intra-FVIII interactions by examining effects of mutations at the A3–C1 and C1–C2 domain interfaces, localized within the single-chain A3C1C2 subunit. Results from this study show differential effects upon placement of an additional covalent linkage, in the form of a nascent disulfide bridge, at the A3–C1 domain interface. Residue pairings for mutagenesis to Cys were chosen on the basis of residue Cα spatial separations of ∼5–7 Å. While the Gly1750Cys/Arg2116Cys variant showed an ∼3–4-fold increase in FVIII thermal stability that was accompanied by a modest increase in FVIIIa stability, the Ala1866Cys/Ser2119Cys FVIII variant decayed at a rate nearly 5 times the WT FVIII value at elevated temperatures. Thus constraints imposed by the disulfide bonds at this interface show markedly disparate effects. Furthermore, the positive charge of Arg2116 appears to directly contribute to the interface stability based upon reductions in this and other parameter values when this residue is replaced with Ala or Val. Finally, mutation to place a nascent disulfide bridge at the C1–C2 interface (Ser2029Cys/Pro2292Cys) resulted in a marked reduction in FVIII thermal stability. However, this FVIII variant showed a modest increase in specific activity, possibly as a result of improved interaction of the cofactor with substrate FX.

dx.doi.org/10.1021/bi400295x | *Biochemistry* 2013, 52, 3921–3929

It is not surprising that one of the mutants (Gly1750Cys/Arg2116Cys) with a nascent disulfide bridge at the A3−C1 interface increased FVIII thermal stability. In an earlier study, we showed that introduction of a disulfide bridge by the Arg121Cys/Leu2302Cys mutation at the A1−C2 domain interface resulted in a 3-fold reduction in the rate of FVIII decay at elevated temperatures relative to that of WT FVIII.[17] Our current findings suggest that noncovalent interactions at the A3−C1 domain interface contribute to the overall FVIII structural integrity. Thus, applying additional strength to this interaction by creation of a disulfide bridge at this site increased FVIII stability. In addition, the Gly1750Cys/Arg2116Cys variant showed a modest increase in FVIIIa stability. This effect may be explained by observations that the A2 domain interacts with both A1 and A3 domains, and that A3 is supported by both A1 and C1 domains to interact optimally with the A2 domain. Therefore, we speculate that the stabilization of the A3 domain relative to the C1 domain may cause a favorable effect on A2 domain binding in FVIIIa. However, we also observed that this increase in FVIII stability by fixing the A3−C1 domain interface appeared to be characteristic of a specific interdomain residue pairing based upon the disparate effects noted for the Gly1750Cys/Arg2116Cys and Ala1866Cys/Ser2119Cys variants. The reason(s) for the low stability of the Ala1866Cys/Ser2119Cys variant is not known, but the concurrent low activity of this variant suggests that the nascent disulfide bridge imposed a non-native structural constraint that was detrimental to function.

On the other hand, while the stability of the Ser2029Cys/Pro2292Cys (C1−C2 bridge) FVIII variant was reduced, this variant retained essentially WT-like, if not somewhat increased, activity. Thus, any global structural change due to mutation was unlikely. It is possible that constraints imposed by bridging of the C1−C2 domain interface caused a negative effect(s) at other, more distal interfaces leading to a loss of stability. We attempted to test this alternative by preparing an FVIII mutant with disulfide bridging at both the A1−C1 domain interface and the C1−C2 domain interface. That mutant (FVIII Arg121Cys/Leu2302Cys/Ser2029Cys/Pro2292Cys) possessed an efficient linkage between the C1 and C2 domains based upon SDS−PAGE. However, there was only partial bridging (<50%) at the A1−C2 domain interface as judged by free A1 and A3C1C2 subunits compared with the dithiothreitol-resistant A1/A3C1C2 dimer (data not shown). This result was unexpected because the FVIII Arg121Cys/Leu2302Cys variant had previously shown essentially complete disulfide bond formation.[17] This observation suggests that the altered A1−C2 domain interaction that limited bridging in the double disulfide bond variant resulted from a constraint imposed by bridging at the C1−C2 interface. Although limited information could be derived for this variant because of incomplete bridging, the thermal stability of the doubly disulfide-bridged mutant was reduced to a lesser extent (1.6-fold relative to that of the WT; results not shown) than that of the C1−C2 bridged variant (3.7-fold relative to that of the WT). Thus, we speculate that the decreased thermal stability of the C1−C2 bridged variant results from other, more distal alterations such as a possible change at the A1−C2 domain interface.

Interestingly, adding a disulfide bridge to the C1−C2 domain interface in the FVIII Ser2029Cys/Pro2292Cys variant modestly improved FVIII activity in a one-stage clotting assay and thrombin generation potential but not the activity measured in a two-stage FXa generation assay. We speculate these results derive from an enhanced interaction of the variant FVIII with FX. The one-stage clotting and thrombin generation assays use diluted plasma as a source of FX; thus, the substrate is not at the V_{max} concentration, unlike the two-stage FXase assay that uses purified proteins, including a V_{max} concentration of the FX substrate. Thus, the reduced K_m would increase the catalytic efficiency of FXase with limiting substrate in the plasma-based assays. Furthermore, affinity values of the WT and Ser2029Cys/Pro2292Cys FVIII variant for FIXa were quite similar. In addition, experiments measuring the fluorescence anisotropy of fluorescein-Phe-Phe-Arg FIXa (fl-FFR-FIXa) showed no change in anisotropy values upon comparison of the WT and variant FVIII. However, the increase in anisotropy following addition of FX to the FXase complex was somewhat faster for FXase comprised of mutant FVIIIa than for that comprised of WT FVIIIa (data not shown), suggesting that the association rate for FX was increased with the variant cofactor. Because the C2 domain is reported to form a part of the binding sites for FXa and FIXa,[25−27] it is not surprising that enhanced structural stabilization of the C2−C1 boundary could improve the interprotein interactions. To the best of our knowledge, this is the first report of the generation of an FVIII variant with increased FX affinity.

Results from the mutagenesis of Arg2116 suggest this residue contributes to the binding energy at the A3−C1 domain interface. As suggested by the intermediate-resolution (3.98 Å) FVIII X-ray crystal structure,[8] the side chain of Arg faces a strong positive charge in the A3 domain from the amide nitrogen from Gly1750 and from the side chain of Arg1749 (Figure 1, bottom right panel). Thus, one would predict this interaction to be destabilizing. However, experimental results eliminating this charge following replacement of Arg2116 with Ala or Val yielded reductions in FVIII stability. These results suggest the presumed location of the Arg2116 side chain may not be accurate. We note that the acidic side chain of Glu1751 appears to be in the proximity of Arg2116 (Cα distance of 6.18 Å). Thus, we speculate that the side chain of Arg2116 may be in an appropriate position to accommodate an electrostatic interaction with Glu1751.

Our results from several studies examining FVIII and FVIIIa stability following a selected mutation at each domain interface have yielded several general observations. Enhancing the affinity of the A2 subunit of FVIIIa for the A1/A3C1C2 dimer by replacing destabilizing charged residues in hydrophobic pockets at the A1−A2 and A2−A3 domain interfaces shows clear correlations with increased specific activity, thermal stability, and thrombin generation parameters.[15,16] These improved activity and thrombin generation values are consistent with earlier studies in which the A2 domain was covalently linked to other FVIII domains by disulfide bridging.[18,19] On the other hand, modifications to improve stability at interfaces not involving the A2 domain [A1−C2[17] and A3−C1 and C1−C2 (this study)] show variable effects on the thermal stability of FVIII and minimal effects on the decay of FVIIIa. Nascent disulfide bonds with the Arg121Cys/Leu2302Cys (A1−C2)[17] and Gly1750Cys/Arg2116Cys [A3−C1 (this study)] mutations resulted in ∼3-fold reductions in the rate of FVIII decay at elevated temperatures, whereas the Ala1866Cys/Ser2119Cys (A3−C1) and Ser2029Cys/Pro2292Cys (C1−C2) variants in this study showed marked decreases in thermal stability. Thus, non-native covalent linkages can be clearly detrimental to protein structure.

However, we note that under conditions used for activity measurements such as specific activity and thrombin generation parameter values, the FVIII thermal stability parameter value does not necessarily correlate with these activity parameters.

AUTHOR INFORMATION

Corresponding Author

*Department of Biochemistry and Biophysics, University of Rochester School of Medicine, 601 Elmwood Ave., Rochester, NY 14642. E-mail: philip_fay@urmc.rochester.edu. Phone: (585) 275-6576.

Funding

This work was supported by National Institutes of Health Grants HL38199 and HL76213.

Notes

The authors declare no competing financial interest.

ACKNOWLEDGMENTS

We thank Lisa M. Regan of Bayer Corp. for the gifts of recombinant human FVIII and anti-FVIII antibody (2D2) and Pete Lollar and John Healey for the FVIII cloning and expression vectors.

ABBREVIATIONS

WT, wild type; FVIII, factor VIII; FX, factor X; FIXa, factor IXa; FXase, factor Xase; SDS−PAGE, sodium dodecyl sulfate−polyacrylamide gel electrophoresis; ETP, endogenous thrombin potential.

REFERENCES

(1) Fay, P. J. (2004) Activation of factor VIII and mechanisms of cofactor action. *Blood Rev. 18*, 1−15.

(2) Fay, P. J. (1988) Reconstitution of human factor VIII from isolated subunits. *Arch. Biochem. Biophys. 262*, 525−531.

(3) Wakabayashi, H., Koszelak, M. E., Mastri, M., and Fay, P. J. (2001) Metal ion-independent association of factor VIII subunits and the roles of calcium and copper ions for cofactor activity and inter-subunit affinity. *Biochemistry 40*, 10293−10300.

(4) Wakabayashi, H., Freas, J., Zhou, Q., and Fay, P. J. (2004) Residues 110−126 in the A1 domain of factor VIII contain a Ca^{2+} binding site required for cofactor activity. *J. Biol. Chem. 279*, 12677−12684.

(5) Wakabayashi, H., Zhou, Q., Nogami, K., Ansong, C., Varfaj, F., Miles, S., and Fay, P. J. (2006) pH-dependent association of factor VIII chains: Enhancement of affinity at physiological pH by Cu^{2+}. *Biochim. Biophys. Acta 1764*, 1094−1101.

(6) Ansong, C., and Fay, P. J. (2005) Factor VIII A3 Domain Residues 1954−1961 Represent an A1 Domain-Interactive Site. *Biochemistry 44*, 8850−8857.

(7) Shen, B. W., Spiegel, P. C., Chang, C. H., Huh, J. W., Lee, J. S., Kim, J., Kim, Y. H., and Stoddard, B. L. (2008) The tertiary structure and domain organization of coagulation factor VIII. *Blood 111*, 1240−1247.

(8) Ngo, J. C., Huang, M., Roth, D. A., Furie, B. C., and Furie, B. (2008) Crystal structure of human factor VIII: Implications for the formation of the factor IXa-factor VIIIa complex. *Structure 16*, 597−606.

(9) Fay, P. J., Haidaris, P. J., and Smudzin, T. M. (1991) Human factor VIIIa subunit structure. Reconstruction of factor VIIIa from the isolated A1/A3-C1-C2 dimer and A2 subunit. *J. Biol. Chem. 266*, 8957−8962.

(10) Lollar, P., and Parker, C. G. (1990) pH-dependent denaturation of thrombin-activated porcine factor VIII. *J. Biol. Chem. 265*, 1688−1692.

(11) Lollar, P., and Parker, E. T. (1991) Structural basis for the decreased procoagulant activity of human factor VIII compared to the porcine homolog. *J. Biol. Chem. 266*, 12481−12486.

(12) Fay, P. J., Beattie, T. L., Regan, L. M., O'Brien, L. M., and Kaufman, R. J. (1996) Model for the factor VIIIa-dependent decay of the intrinsic factor Xase. Role of subunit dissociation and factor IXa-catalyzed proteolysis. *J. Biol. Chem. 271*, 6027−6032.

(13) Wakabayashi, H., and Fay, P. J. (2008) Identification of Residues Contributing to A2 Domain-dependent Structural Stability in Factor VIII and Factor VIIIa. *J. Biol. Chem. 283*, 11645−11651.

(14) Sammond, D. W., Eletr, Z. M., Purbeck, C., Kimple, R. J., Siderovski, D. P., and Kuhlman, B. (2007) Structure-based protocol for identifying mutations that enhance protein-protein binding affinities. *J. Mol. Biol. 371*, 1392−1404.

(15) Wakabayashi, H., Varfaj, F., Deangelis, J., and Fay, P. J. (2008) Generation of enhanced stability factor VIII variants by replacement of charged residues at the A2 domain interface. *Blood 112*, 2761−2769.

(16) Wakabayashi, H., Griffiths, A. E., and Fay, P. J. (2009) Combining mutations of charged residues at the A2 domain interface enhances factor VIII stability over single point mutations. *J. Thromb. Haemostasis 7*, 438−444.

(17) Wakabayashi, H., Griffiths, A. E., and Fay, P. J. (2011) Increasing hydrophobicity or disulfide bridging at the factor VIII A1 and C2 domain interface enhances procofactor stability. *J. Biol. Chem. 286*, 25748−25755.

(18) Pipe, S. W., and Kaufman, R. J. (1997) Characterization of a genetically engineered inactivation-resistant coagulation factor VIIIa. *Proc. Natl. Acad. Sci. U.S.A. 94*, 11851−11856.

(19) Gale, A. J., and Pellequer, J. L. (2003) An engineered interdomain disulfide bond stabilizes human blood coagulation factor VIIIa. *J. Thromb. Haemostasis 1*, 1966−1971.

(20) Mimms, L. T., Zampighi, G., Nozaki, Y., Tanford, C., and Reynolds, J. A. (1981) Phospholipid vesicle formation and transmembrane protein incorporation using octyl glucoside. *Biochemistry 20*, 833−840.

(21) Doering, C., Parker, E. T., Healey, J. F., Craddock, H. N., Barrow, R. T., and Lollar, P. (2002) Expression and characterization of recombinant murine factor VIII. *Thromb. Haemostasis 88*, 450−458.

(22) Wakabayashi, H., Su, Y. C., Ahmad, S. S., Walsh, P. N., and Fay, P. J. (2005) A Glu113Ala Mutation within a Factor VIII Ca^{2+}-Binding Site Enhances Cofactor Interactions in Factor Xase. *Biochemistry 44*, 10298−10304.

(23) Hemker, H. C., Giesen, P., Al Dieri, R., Regnault, V., de Smedt, E., Wagenvoord, R., Lecompte, T., and Beguin, S. (2003) Calibrated automated thrombin generation measurement in clotting plasma. *Pathophysiol. Haemostasis Thromb. 33*, 4−15.

(24) Ansong, C., Miles, S. M., and Fay, P. J. (2006) Factor VIII A1 domain residues 97−105 represent a light chain-interactive site. *Biochemistry 45*, 13140−13149.

(25) Nogami, K., Shima, M., Hosokawa, K., Suzuki, T., Koide, T., Saenko, E. L., Scandella, D., Shibata, M., Kamisue, S., Tanaka, I., and Yoshioka, A. (1999) Role of factor VIII C2 domain in factor VIII binding to factor Xa. *J. Biol. Chem. 274*, 31000−31007.

(26) Ahmad, S. S., and Walsh, P. N. (2005) Role of the C2 domain of factor VIIIa in the assembly of factor-X activating complex on the platelet membrane. *Biochemistry 44*, 13858−13865.

(27) Soeda, T., Nogami, K., Nishiya, K., Takeyama, M., Ogiwara, K., Sakata, Y., Yoshioka, A., and Shima, M. (2009) The factor VIIIa C2 domain (residues 2228−2240) interacts with the factor IXa Gla domain in the factor xase complex. *J. Biol. Chem. 284*, 3379−3388.